Extraordinary optical transmission through a subwavelength composite hole-pillar array*

Shao Wei-Jia(邵伟佳)[a)b)], Li Wei-Min(李为民)[a)†], Xu Xiao-Liang(许小亮)[b)‡], Wang Hui-Jie(王会杰)[b)], Wu Yi-Zhi(吴以治)[b)], and Yu Jing (郁 菁)[b)]

[a)] *National Synchrotron Radiation Laboratory and School of Nuclear Science and Technology, University of Science and Technology of China, Hefei* 230026, *China*

[b)] *Department of Physics, University of Science and Technology of China, Hefei* 230026, *China*

(Received 21 April 2014; revised manuscript received 21 May 2014; published online 24 September 2014)

We numerically investigate the transmission properties of a subwavelength composite hole-pillar array. As the radius of the pillar increases, the transmission properties experience a complex evolution. It is found that the magnetic dipole resonance of the pillar suppresses the surface plasmon polariton resonance (SPPR) at the gold-air interface. There are two strong transmission peaks associated with the magnetic dipole resonance of pillar and SPPR at the gold-silica interface. A peak associated with magnetic quadrupole resonance of the pillar is observed. Moreover, there is a weak peak associated with the coupling between the whispering-gallery plasmon (WGP) mode and magnetic dipole. Our work is helpful for making a dual band optical filter.

Keywords: surface plasmon polariton resonance (SPPR), transmission, optical filter

PACS: 73.20.Mf, 42.79.Ci **DOI:** 10.1088/1674-1056/23/11/117301

1. Introduction

In 1998, Ebbesen *et al*. first reported the extraordinary optical transmission (EOT) through a silver film perforated by a two-dimensional (2D) array of subwavelength holes in the visible and infrared regions.[1] They found that the transmission through a metallic subwavelength hole array can significantly exceed the value predicted by Beth's theory. Although some different interpretations still exist,[2–4] it is well known that surface plasmon polariton resonance (SPPR) is involved in EOT.[5]

It has been confirmed that there are three mechanisms involved in EOT. Firstly, under the action of the electric field of incident light, the free electrons in the metal surface collectively oscillate. SPPR originates from the resonant coupling between the incident light and collective oscillation of the free electrons at the metal-dielectric interface.[6] SPPR leads to the electric field enhancement in the hole, thus the enhanced transmission. Secondly, localized surface plasmons (LSPs) are usually excited by the incident light for isolated subwavelength conductive nanoparticles, which leads to field amplification both inside and outside the particle in the near field zone.[7] The LSP can also be excited in a penetrating hole, therefore, LSP of the holes is involved in EOT.[8,9] Thirdly, a penetrating hole in a metal film can be treated as a waveguide, so the intrinsic electromagnetic modes from the holes can also lead to EOT.[10] It is worth noting that the first mechanism may interact with the other two.[11,12] In some situations, these interactions may lead to a confusing of the essence of the EOT.

Actually, EOT has been demonstrated in the different bands of the electromagnetic spectrum as long as there are resonances, such as split ring resonance,[13,14] or LC resonance.[15] Many efforts have been devoted to exploring the physics behind EOT. Recently, the magnetic resonances of dielectric particles with high permittivity have aroused considerable interest in the visible and infrared regions.[16–18] It is natural to explore the effect of the magnetic resonances of dielectric particles on the EOT.

In the present work, we numerically study how the magnetic resonances of silicon pillars affect EOT in the composite hole-pillar structure by considering only the first mechanism. This is reasonable because the radius in our study is small enough to avoid the waveguide effect. Moreover, the LSP effect usually occurs in a sharp rectangle hole[8] or in an anistropic three-dimensional (3D) hole.[9] As is well known, the optical transmission of some analogous composite structures has been investigated.[19–23] To the best of our knowledge, the present study is the first report about the effect of the magnetic resonances on the EOT. Remarkably, the magnetic resonances of silicon pillars mediate the transmission properties of the studied structure. Moreover, our structure can be utilized to make dual band optical filters.

*Project supported by the National Natural Science Foundation of China (Grant No. 51272246) and the Scientific and Technological Research Foundation of Anhui Province, China (Grant No. 12010202035).

†Corresponding author. E-mail: lwm@ustc.edu.cn

‡Corresponding author. E-mail: xlxu@ustc.edu.cn

© 2014 Chinese Physical Society and IOP Publishing Ltd

2. Structure and simulation model

As schematic is shown in Fig. 1(a), a patterned gold film with a thickness of 200 nm is deposited on a silica substrate. The gold film is perforated by a square array of cylindric air holes. A cylindric silicon pillar is located in the center of each hole. Figure 1(b) illustrates the parameters of the composite structure unit cell in the center section parallel to the x–z plane. The radius of the hole is 100 nm and the periodicity of the array is 400 nm. The radius of the silicon pillar is denoted by r. The height of the silicon pillar is 200 nm. The incident light normally irradiates the patterned film from the silica side (along the z direction). The wavelength of the incident light is chosen from 500 nm to 1100 nm. The incident light is linearly polarized along the x direction.

We used commercial package FDTD solutions obtained from Lumerical Inc. to simulate the transmission of the studied composite hole-pillar structure. In the optical simulations, the refractivity of the silica was set to be 1.5. The permitivity of the gold was cited from the experimental data given by Johnson and Christy.[24] The data in Palik's handbook was used to fit the permittivity curve of the silicon.[25] Figure 1(c) shows the schematic of the FDTD simulation model. In the simulation model, perfectly matched layer boundary conditions were used in the incident direction to prevent the interference effect, and periodic boundary conditions were used in the lateral direction to simulate the composite hole-pillar structures. A light source was located in the silica substrate to simulate the incident light, and a transmission monitor was used to collect the transmission light and calculate the transmission spectrum.

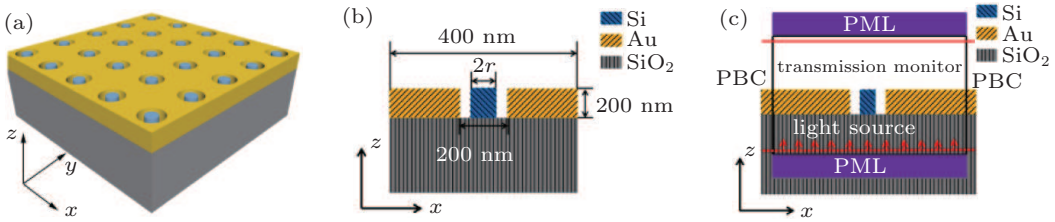


Fig. 1. (color online) (a) Schematic diagram of the studied composite hole-pillar structure. (b) Parameters of the composite structure unit cell in the center section parallel to the x–z plane. The radius of the silicon pillar is denoted by r. (c) Schematic diagram of the FDTD simulation model. PML: perfectly matched layer, PBC: periodic boundary condition.

The studied composite hole-pillar structure can be fabricated through some micro-nano technologies. First, we deposited the gold film on a silica substrate, and we then wrote the hole array in the gold film by the focused iron beam (FIB) method. After fabricating the metallic hole array, we deposited the silicon in the hole and onto the gold film. It is convenient to fabricate a composite hole-pillar structure using the reactive iron etching (RIE) method.

3. Results and discussion

Figures 2(a) and 2(b) show the transmission spectra of the composite hole-pillar structure with different values of r. The transmission of the simple hole array without pillar array is also shown as a reference (solid lines). In each reference line, there are two peaks at 570 nm and 684 nm. Since the incident light irradiates the simple hole array without pillar array, the incident light excites the SPPR at the metal-dielectric interface. The two peaks of reference line are associated with two different SPPRs. According to Ref. [26], the peak with a longer wavelength is associated with SPPR at the gold-silica interface and the peak with shorter wavelength is related to SPPR at gold-air interface.

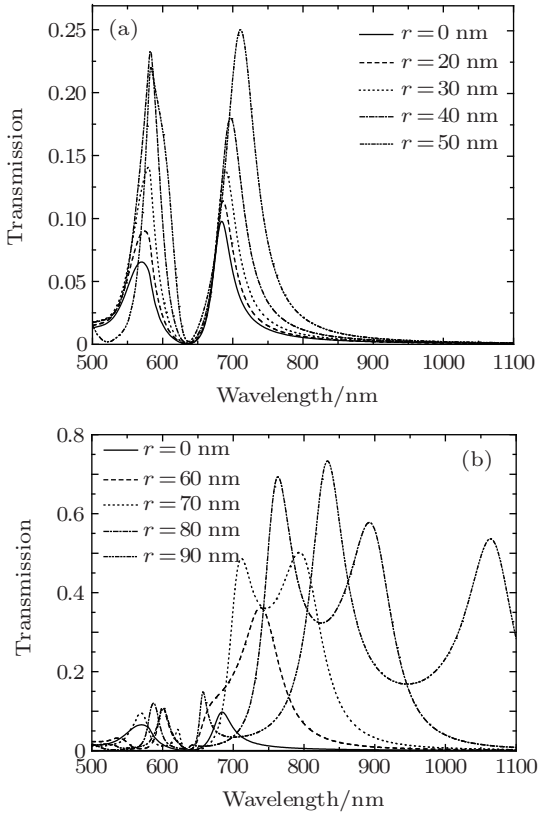


Fig. 2. Transmission spectra of the composite hole-pillar structure as r increases from (a) 20 nm to 50 nm and from (b) 60 nm to 90 nm in steps of 10 nm. The transmission spectrum of the simple hole array without pillar array is also plotted as a reference (solid lines in panels (a) and (b)).

Both the values of the transmission peaks of the reference line are less than 0.1. As r increases from 20 nm to 50 nm, these two transmission peaks are enhanced and they shift toward longer wavelengths. However, there is an exception as r increases from 40 nm to 50 nm, where the transmission peak with the short wavelength is suppressed. The details of this suppression are discussed below. The transmission properties of this composite structure are totally different when $r = 60$ nm. Besides a bump near 670 nm, there are three peaks at 536 nm, 600 nm, and 738 nm. It is suggested that the bump is a peak which is covered up by the peak at 738 nm. As r increases, all of these four peaks shift toward longer wavelengths. It is worth noting that the ratio of the hole area to the cell area is only 0.193. However, as $r = 80$ nm, the values of transmission peaks at 763 nm and 892 nm are 0.694 and 0.578, respectively. The transmissions are enhanced by three times compared with 0.193. This is an advantage to utilize this property to make dual band optical filter.

There are four transmission peaks, respectively, at 570, 622, 712, and 793 nm when r = 70 nm. The peaks at 793 and 712 nm are strong and the peaks at 570 and 622 nm are weak. In order to gain an insight into the composite hole-pillar structure, the basic physical essence of the four peaks

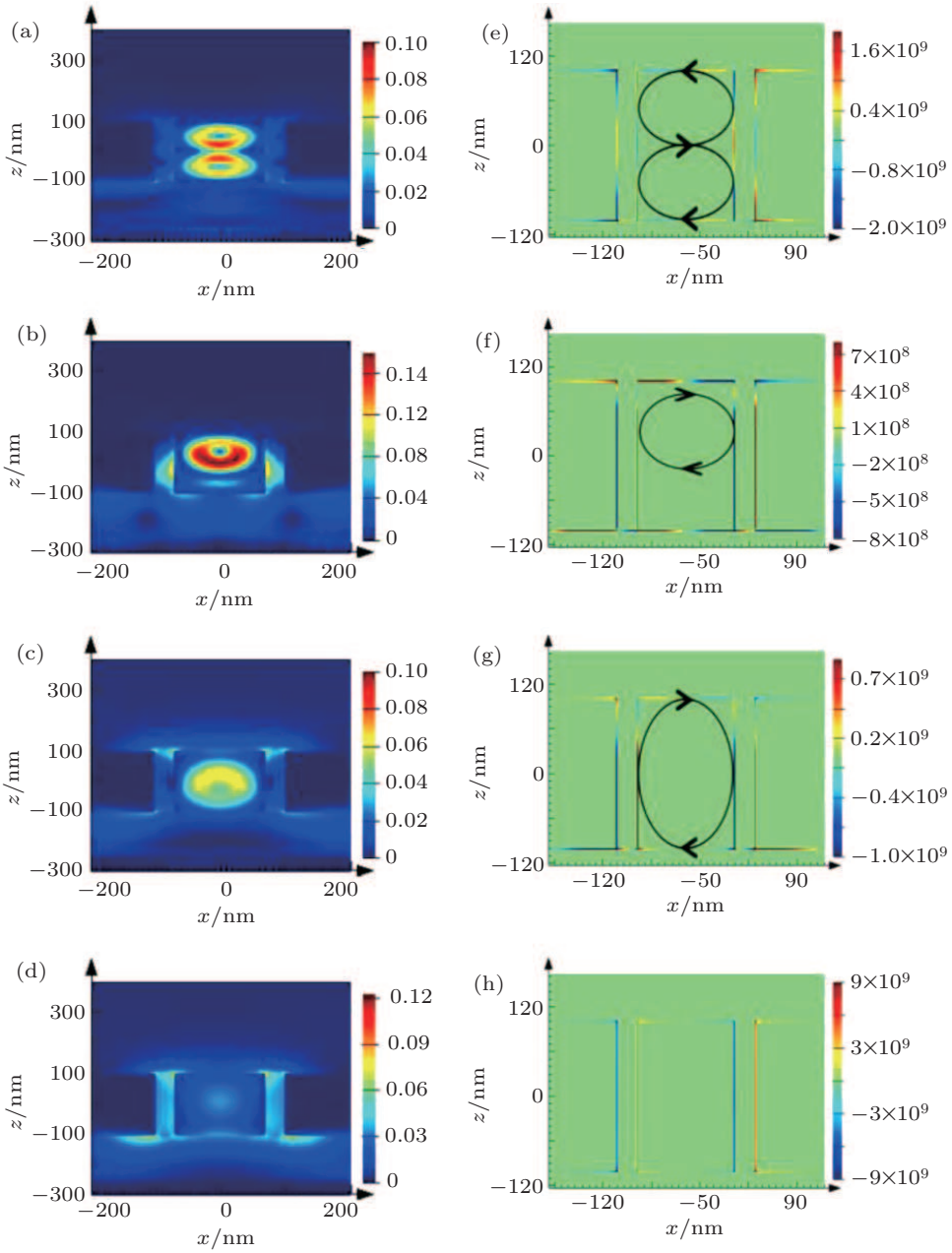


Fig. 3. (color online) The calculated magnitudes of the Poynting vector in the center section of the composite structure unit cell parallel to the x–z plane for the incident light wavelengths of (a) 570 nm, (b) 622 nm, (c) 712 nm, and (d) 793 nm at $r = 70$ nm. The calculated divergences of the electric field in the center section of the composite structure unit cell parallel to the x–z plane for incident light wavelengths of (e) 570 nm, (f) 622 nm, (g) 712 nm, and (h) 793 nm at $r = 70$ nm.

should be investigated. We plot the color maps of the magnitude of the poynting vectors at 570, 622, 712, and 793 nm in the center section parallel to the x–z plane when $r = 70$ nm as shown in Figs. 3(a)–3(d), respectively. Furthermore, according to Gauss's law, in which the divergence of the electric field is proportional to the polarization charge density, we illustrate the divergences of the electric field at 570, 622, 712, and 793 nm in the center section parallel to the x–z plane when $r = 70$ nm in Figs. 3(e)–3(h), respectively. Figure 3(a) indicates the existence of a magnetic quadrupole resonance of the silicon pillar. Figure 3(e) shows that magnetic quadrupole is composed of two loop polarization currents. The polarization current originates from the aggregation of polarization charge with opposite signs at the boundary of the silicon pillar, as shown in Fig. 3(e). The direction of the polarization current is set to be from the negative charge to the positive charge. The loop polarization current is composed of two polarization currents with opposite directions. As a result, the weak peak at 570 nm is associated with the magnetic quadrupole resonance of the silicon pillar. Figure 3(b) shows that, when the incident light with a wavelength of 622 nm irradiates the composite hole-pillar structure, some energy of the incident light is trapped in the gap between the silicon pillar and the inwall of the hole. This is a clue to whispering gallery plasmon (WGP) mode.[27] When radius of the hole is subwavelength, the WGP mode cannot be excited. However, it is suggested that inserting a dielectric with high permittivity (such as silicon) increases the optical radius of the hole, thus exciting the WGP mode. Once the WGP is excited, the energy of the incident light is trapped in the hole. This is why the transmission peak at 622 nm is weak. Additionally, figure 3(b) exhibits the characteristics of a magnetic dipole. Figure 3(f) also shows a magnetic dipole, which is composed of a loop polarization current. Consequently, the peak at 622 nm is associated with the coupling between the magnetic dipole and WGP mode. The profile of the magnitude of poynting vector in Fig. 3(c) obviously indicates the existence of a magnetic dipole resonance. Figure 3(g) shows that the incident light with a wavelength of 712 nm excites a magnetic dipole resonance, which is composed of a loop polarization current. As a result, the strong peak at 712 nm is associated with the magnetic dipole resonance of the silicon pillar. Figure 3(d) shows that the electromagnetic energy propagates along the gap between the pillar and inwall of the hole. The incident light with a wavelength of 793 nm barely interacts with the silicon pillar. Figure 3(h) shows the conventional distribution of the polarization charge under the action of an external electric field. It is suggested that the peak at 793 nm is associated with SPPR at the gold-silica interface.

To find the suppression of the transmission peak with shorter wavelength when the radius of the pillar increases from 40 nm to 50 nm, the calculated magnitudes of the poynting vectors in the center section of the unit cell parallel to the x–z plane are plotted in Figs. 4(a) and 4(b). When r= 40 nm, the electromagnetic energy propagates along the gap between the pillar and inner wall of the hole as the wavelength of the incident light is 582 nm (see Fig. 4(a)). At $r = 50$ nm, figure 4(b) shows that the poynting vector in the silicon pillar is significant at 582 nm, which is represented by the magnetic dipole resonance of the silicon pillar. The Poynting vector in the gap of Fig. 4(b) is reduced compared with that of Fig. 4(a), especially that near the top surface of the gold film. Thus, it is suggested that the magnetic dipole resonance of the silicon pillar suppresses the SPPR at the gold-air interface. Consequently, the transmission is reduced compared with the scenario at $r = 40$ nm (shown in Fig. 2(a)). It is suggested that the case for $r = 50$ nm is a critical change point because when $r = 50$ nm, the magnetic resonances of silicon pillars start to mediate the transmission properties of the composite structure. Furthermore, the peak at 582 nm for $r = 50$ nm is composed of two peaks associated with SPPR at the gold-air interface and the magnetic dipole resonance of the silicon pillars.

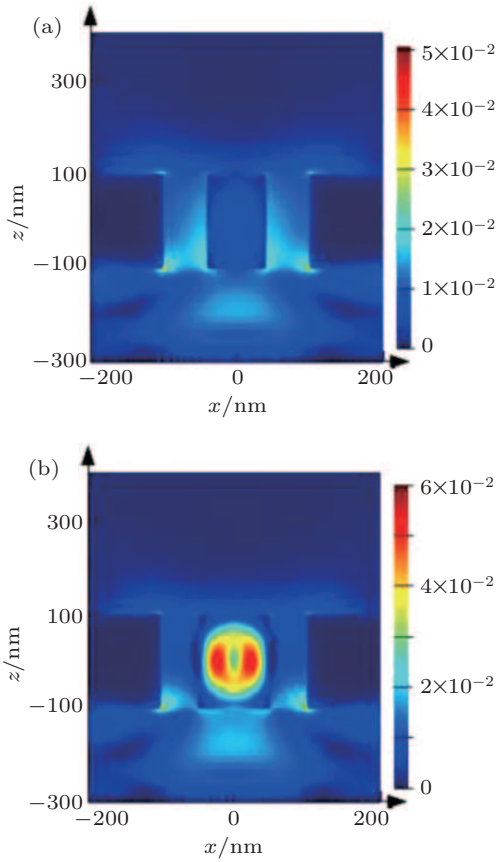


Fig. 4. (color online) Calculated magnitudes of Poynting vector in the center section of the unit cell parallel to the x–z plane as $r = 40$ nm (a) and 50 nm (b) at 582 nm.

When $r = 70$ nm, figures 5(a) and 5(b) show the magnitudes of the electric fields, respectively, on the gold-air and gold-silica interfaces in the cross section of the unit cell as the

wavelength of the incident light is 712 nm. Obviously, the electric field is enhanced in the gap between the pillar and in the wall of the hole. The enhanced field indicates the coupling between the magnetic dipole resonance and SPPR, which is similar to the coupling between the electric dipole resonance and the SPPR.[18]

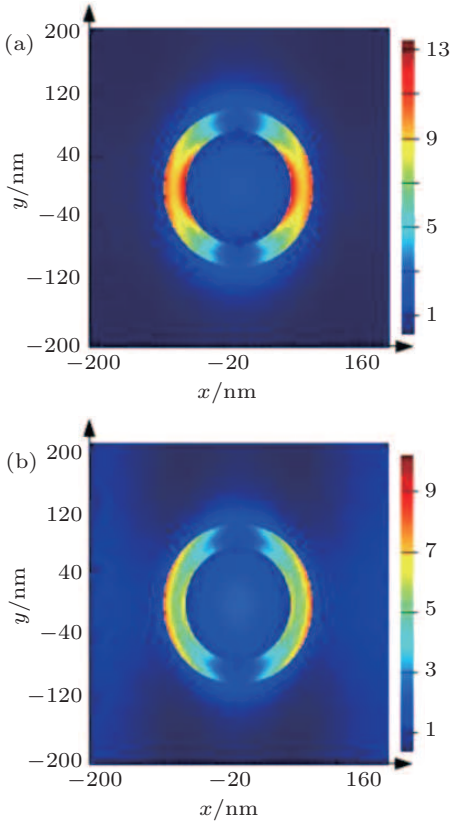


Fig. 5. (color online) Calculated magnitudes of the electric field on the (a) gold-air and (b) gold-silica interface in the cross section of the unit cell when $r = 70$ nm at 712 nm.

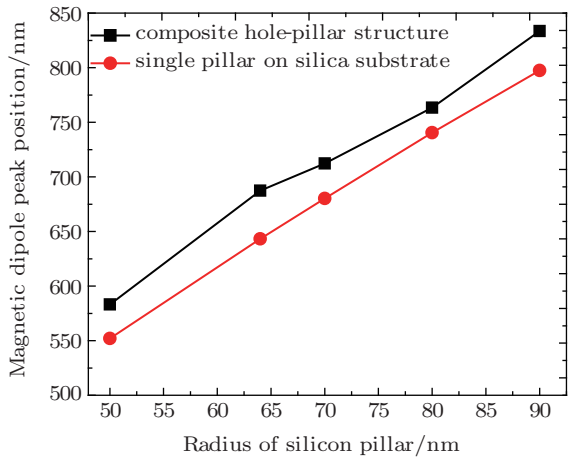


Fig. 6. (color online) Variations of the peak position of the magnetic dipole resonance of composite hole-pillar structure (solid square) and single silicon pillar (solid circle) deposited on a silica substrate with radius of the silicon pillar in a range from 64 nm to 90 nm.

Actually, a single silicon pillar deposited on a silica substrate also exhibits magnetic dipole resonance.[28] We calculate the position of the magnetic dipole resonance peak of a single silicon pillar deposited on a silica substrate. In the calculation, the incident light normally irradiates the silicon pillar from the silica side. As shown in Fig. 6, the energy of the magnetic dipole resonance peak of the composite hole-pillar structure is lower than that of same single pillar deposited on a silica substrate. It is suggested that the red shift between the peaks associated with magnetic dipole resonances of composite hole-pillar structure and single pillar deposited on silica substrate is due to the coupling between the magnetic dipole resonance and SPPR.

It is found that both the SPPR at the gold-silica interface and the magnetic dipole resonance show red-shift with the increase of r. As r increases, because of the introduction of the silicon pillar, the effective refractive index of the silica substrate increases, leading to the red shift of the SPPR peak. Additionally, as r increases, the energy of the magnetic dipole resonance is suppressed, leading to the red shift of the magnetic dipole peak.[28]

4. Summary

In this paper, we numerically investigate the transmission of a composite structure of a periodic hole-pillar array. As r increases, the transmission properties of the composite structure experience an evolution from simple to complex. As $r < 40$ nm, two peaks associated with two SPPRs at the gold-air and gold-silica interfaces are enhanced, they also shift towards longer wavelengths. When $r > 50$ nm, the magnetic dipole resonance of the silicon pillar suppresses the SPPR at the gold-air interface. As $r > 60$ nm, the magnetic quadrupole resonance of the silicon pillar is observed. Additionally, there is a weak peak associated with the coupling between the WGP mode and magnetic dipole. It is found the electric resonances of the silicon pillars do not make contributions to the transmission of the composite structure. Our work not only reveals the effects of the magnetic resonance on the EOT but is also helpful to the design of tunable dual band optical filters.

References

[1] Ebbesen T W, Lezec H J, Ghaemi H F, Thio T and Wolff P A 1998 *Nature* **391** 667
[2] Lalanne P and Hugonin J P 2006 *Nat. Phys.* **2** 551
[3] Gay G, Alloschery O, Viaris de Lesegno B, O'Dwyer C, Weiner J and Lezec H J 2006 *Nat. Phys.* **2** 262
[4] Visser T D 2006 *Nat. Phys.* **2** 509
[5] Wei F F, Wang H Y and Zhou Y S 2013 *Chin. Phys. B* **22** 024201
[6] Barnes W L, Dereux A and Ebbesen T W 2003 *Nature* **424** 824
[7] Wang F and Shen Y R 2006 *Phys. Rev. Lett.* **97** 206806
[8] Klein K K J, Enoch S, Segerink F B, van Hulst N F and Kuipers L 2004 *Phys. Rev. Lett.* **92** 183901
[9] Yang J C, Gao H, Suh J Y, Zhou W, Lee M H and Odom T W 2010 *Nano Lett.* **10** 3173
[10] Ruan Z and Qiu M 2006 *Phys. Rev. Lett.* **96** 233901
[11] Bao Y J, Peng R W, Shu D J, Wang M, Lu X, Shao J, Lu W and Ming N B 2008 *Phys. Rev. Lett.* **101** 087401
[12] Miyamaru F and Takeda M W 2009 *Phys. Rev. B* **79** 153405

[13] Cakmak A O, Aydin K, Colak E, Li Z, Bilotti F, Vegni L and Ozbay E 2009 *Appl. Phys. Lett.* **95** 052103

[14] Aydin K, Cakmak A O, Sahin L, Li Z, Bilotti F, Vegni L and Ozbay E 2009 *Phys. Rev. Lett.* **102** 013904

[15] Xiao S, Peng L and Mortensen N A 2010 *Opt. Express* **18** 6040

[16] Evlyukhin A B, Novikov S M, Zywietz U, Eriksen R L, Reinhardt C, Bozhevolnyi S I and Chichkov B N 2012 *Nano Lett.* **12** 3749

[17] García-Etxarri A, Gómez-Medina R, Froufe-Pérez L S, López C, Chantada L, Scheffold F, Aizpurua J, Nieto-Vesperinas M and Sáenz J J 2011 *Opt. Express* **19** 4815

[18] Ginn J C, Brener I, Peters D W, Wendt J R, Stevens J O, Hines P F, Basilio L I, Warne L K, Ihlefeld J F, Clem P G and Sinclair M B 2012 *Phys. Rev. Lett.* **108** 097402

[19] Wang C, Gu J, Han J, Xing Q, Tian Z, Liu F, Chai L, Li Y, Hu M, Wang Q, Lu X and Zhang W 2010 *Appl. Phys. Lett.* **96** 251102

[20] Stolwijk D, Driessen E F C, Verschuuren M A, Hooft G W 't, van Exter M P and de Dood M J A 2008 *Opt. Lett.* **33** 363

[21] Poujet Y, Salvi J and Baida F I 2007 *Opt. Lett.* **32** 2942

[22] Lu X and Zhang W 2009 *Appl. Phys. Lett.* **94** 181106

[23] Wu S, Wang Q J, Yin X G, Li J Q, D Zhu, Liu S Q and Zhu Y Y 2008 *Appl. Phys. Lett.* **93** 101113

[24] Johnson P B and Christy R W 1972 *Phys. Rev. B* **6** 4370

[25] Edwards D F 1985 *Handbook of Optical Constants of Solids* (Vol. 1) (Orlando, FL: Academic Press) p. 547

[26] Salomon L, Grillot F, Zayats A V and de Fornel F 2001 *Phys. Rev. Lett.* **86** 1110

[27] Vesseur E J R, Garciía de Abajo F J and Polman A 2009 *Nano Lett.* **9** 3147

[28] Staude I, Miroshnichenko A E, Decker M, Fofang N T, Liu S, Gonzales E, Dominguez J, Luk T S, Neshev D N, Brener I and Kivshar Y 2013 *ACS Nano* **7** 7824